Available online at www.sciencedirect.com
SCIENCE DIRECT®
CARBOHYDRATE RESEARCH
ELSEVIER
Carbohydrate Research 338 (2003) 2913–2919
www.elsevier.com/locate/carres

Note

# Metal ion interactions with sugars. The crystal structure and FT-IR study of the $NdCl_3$–ribose complex

Yan Lu,[a] Guocai Deng,[a,*] Fangming Miao,[b] Zhengming Li[a]

[a] College of Chemistry, Nankai University, Tianjin 300071, PR China
[b] Institute of Crystal Chemistry, Tianjin Normal University, Tianjin 300074, PR China

Received 31 March 2003; received in revised form 22 August 2003; accepted 27 August 2003

**Abstract**

The single-crystal structure of neodymium chloride–ribopyranose pentahydrate, $NdCl_3 \cdot C_5H_{10}O_5 \cdot 5H_2O$ was determined to have $M_r = 490.80$, $a = 9.138(11)$, $b = 8.830(10)$, $c = 9.811(11)$ Å, $\beta = 94.087(18)^\circ$, $V = 789.7(16)$ Å$^3$, $P2_1$, $Z = 2$, $\mu = 0.71073$ Å and $R = 0.0198$ for 2075 observed reflections. The ligand of the title complex was observed in a disordered state and two molecular configurations of $NdCl_3 \cdot C_5H_{10}O_5 \cdot 5H_2O$ were found in the single crystal as a pair of isomers. Both ligand moieties of the two molecules are ribopyranose forms, providing three hydroxyl groups in *ax–eq–ax* orientation for coordination. One ligand of the pair of isomers is β-D-ribopyranose in the $^1C_4$ conformation, and the other is α-D-ribopyranose in the $^4C_1$ conformation. The $Nd^{3+}$ ion is nine-coordinated with five Nd–O bonds from water molecules, three Nd–O bonds from hydroxyl groups of the ribopyranose and one Nd–Cl bond from chloride ion. The hydroxyl groups, water molecules, chloride ions form an extensive hydrogen-bond network. The IR spectral C–C,O–H,C–O and C–O–H vibrations were observed to be shifted in the complex and the IR results are in accordance with those of X-ray spectroscopy.


*Keywords:* D-Ribose; Complexation; Neodymium chloride; Crystal structure; FT-IR

## 1. Introduction

Recent research has shown that the metal-binding properties of carbohydrates have fundamental importance in many biochemical processes, such as the transference and storage of metal ions,[1,2] the action of metal-containing pharmaceuticals, toxic-metal metabolism,[3,4] and $Ca^{2+}$ mediated carbohydrate–protein binding.[5,6] Although coordination chemistry plays a central role in these processes, information regarding the interactions of saccharides with metal cations is rather limited in the literature, especially the detailed three-dimensional structures of the resultant complexes. Most previous work concerning metal–carbohydrate complexes is focused on their aqueous solution chemistry, and relatively few well-characterized solid complexes have been reported, especially for those sugars containing only alcoholic oxygen donor atoms. Only a few crystal structures of such sugar–metal complexes have been determined by X-ray diffraction; these include the D-xylose complex of $Mo^{6+}$,[7] the D-fructose complex of $Ca^{2+}$,[8–10] the D-galactose complex of $Ca^{2+}$,[11] the lactose complex of $Ca^{2+}$,[12] the mannose complex of $Ca^{2+}$,[13] and the D-ribose complex of $Pr^{3+}$,[14] and the roles of metal ions in determining and regulating these structures still remain obscure. Study of the metal ion binding properties of simple carbohydrates should aid in understanding the action of polysaccharides action in the biological processes.

D-Ribose, as a component of nucleic acids, is an important pentose that exists in all organisms, and its metal-ion-binding properties may have biological significance. Solution studies show that D-ribopyranose, having an *ax–eq–ax* sequence of three adjacent hydroxyl groups is readily coordinated with metal cations and forms 1:1 complexes in hydrophilic solvents.[15] The interactions of $Ca^{2+}$, $Sr^{2+}$, $Ba^{2+}$, $La^{3+}$, $Ce^{3+}$, $Pr^{3+}$, $Nd^{3+}$, $Sm^{3+}$, $Eu^{3+}$, $Gd^{3+}$, and $Tb^{3+}$ with D-ribose in

* Corresponding author. Tel.: +86-22-2350-3632.
*E-mail address:* luuyann@vip.sina.com (G. Deng).

0008-6215/03/$ - see front matter © 2003 Elsevier Ltd. All rights reserved.
doi:10.1016/j.carres.2003.08.015

neutral solutions have been studied by NMR and calorimetric methods.[16–18] The ribose–metal complexes of Ti(IV), VO(II), Cr(II), Mn(II), Fe(III), Co(II), Ni(II), Cu(II), Zn(II), Ce(III), Pr(III), and Nd(III) were prepared in strongly alkaline solutions and appropriate structures assigned for the complexes.[19–29] A review on the lanthanide–saccharide complexes has been published by C.P. Rao.[30] However, only one detailed three-dimensional structure of a ribose–metal ion complex, a single crystal of $PrCl_3 \cdot C_5H_{10}O_5 \cdot 5H_2O$, has been reported.[14] In this study, two configurations of $NdCl_3 \cdot C_5H_{10}O_5 \cdot 5H_2O$ are here observed in a single crystal, and are compared with $PrCl_3 \cdot C_5H_{10}O_5 \cdot 5H_2O$. The vibration spectrum of $NdCl_3 \cdot C_5H_{10}O_5 \cdot 5H_2O$ is assigned and interpreted in correlation with the crystal structure.

## 2. Experimental

### 2.1. Materials

$NdCl_3$ was prepared from the corresponding rare earth oxide of high purity (99.99%) and crystallized.[31] D-Ribose was purchased from Acros, and was used without further purification.

### 2.2. Preparation of $NdCl_3 \cdot$ribose$\cdot 5H_2O$

D-Ribose (0.45 g, 3 mmol) and equivalent amounts of neodymium chloride were dissolved in distilled water, and the solution was evaporated slowly until crystallization occurred; yield of purified complex: 71.33%. Anal. Calcd for $NdCl_3 \cdot C_5H_{10}O_5 \cdot 5H_2O$: C, 12.22; H, 4.07; Nd, 29.38. Found: C, 12.04; H, 4.00; Nd, 29.21.

### 2.3. Physical measurements

The mid-IR spectrum was measured on a Nicolet Magna-IR 750 spectrometer using the micro-IR method, 128 scans at 4 $cm^{-1}$ resolution.

A single crystal ($0.30 \times 0.25 \times 0.20$ mm) of $NdCl_3 \cdot$ribopyranose$\cdot 5H_2O$ was mounted on a glass capillary, and data collection was made on a Bruker Smart 1000 diffractometer using monochromatic Mo $K_\alpha$ radiation ($\lambda = 0.71073$ Å) in the $\theta$ range from 2.08 to 25.03° at 293 K. The final cycle of full-matrix, least-squares refinement was based on 2075 observed reflections. Calculations were completed with the SHELX-97 program.

## 3. Results and discussion

### 3.1. X-Ray crystal structure

Two molecular configurations of $NdCl_3 \cdot C_5H_{10}O_5 \cdot 5H_2O$ were observed in the single crystal and these structures are shown together in Fig. 1. Fig. 2 is the projection of the crystal cell in the unit structure of $NdCl_3 \cdot C_5H_{10}O_5 \cdot 5H_2O$ with the $^1C_4$ conformation. The crystal data and structure refinements are listed in Table 1; atomic coordinates and equivalent isotropic displacement parameters in Table 2; selected bond lengths and angles in Table 3.

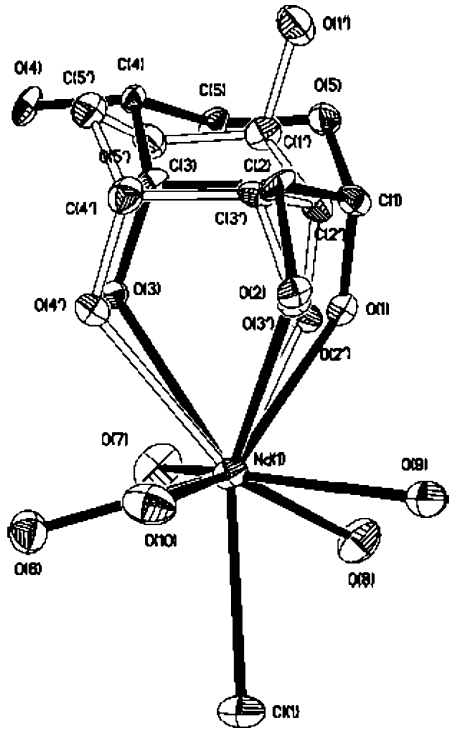


Fig. 1. The structure and atom numbering scheme of $NdCl_3 \cdot C_5H_{10}O_5 \cdot 5H_2O$. The ligand of the complex is in a disordered state, which indicates that there are two configurations of $NdCl_3 \cdot C_5H_{10}O_5 \cdot 5H_2O$ molecules in the single crystal. The one shown by solid bands is α-D-ribopyranose in the $^4C_1$ conformation, and the other shown by hollow bands is β-D-ribopyranose in the $^1C_4$ conformation (labeled by numbers with commas).

The D-ribose moiety of the $NdCl_3 \cdot$ribopyranose$\cdot 5H_2O$ complex is in a disordered state (Fig. 1). This indicates that there are two kinds of $NdCl_3 \cdot C_5H_{10}O_5 \cdot 5H_2O$ molecules in the single crystal, having different configurations. The ribose moiety of one of the molecules is α-pyranose in the $^4C_1$ conformation (shown by solid bands in Fig. 1), and thus resembles $PrCl_3 \cdot$ribose$\cdot 5H_2O$.[14] In the other $NdCl_3 \cdot C_5H_{10}O_5 \cdot 5H_2O$ molecule, the ribose moiety is the β-pyranose in the $^1C_4$ conformation (shown by hollow bands in Fig. 1 and the atoms labeled by numbers with commas), which has not been observed before. The sugar moieties in the two $NdCl_3 \cdot C_5H_{10}O_5 \cdot 5H_2O$ molecules are thus a pair of configurational isomers in 1:1 ratio. In both of the $NdCl_3 \cdot$ribopyranose$\cdot 5H_2O$ molecules, the Nd ion is nine-coordinated and binds to three hydroxyl groups of one D-ribopyranose molecule, five water molecules,

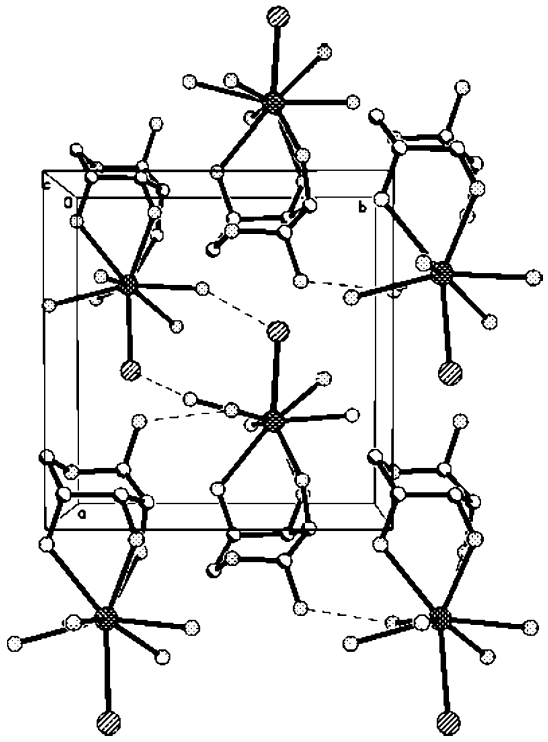

Fig. 2. Projection of the crystal cell in the structure of $NdCl_3 \cdot C_5H_{10}O_5 \cdot 5H_2O$ with the β-ribopyranose $^1C_4$ conformation.

Table 1
Crystal data and structure refinement parameters for $NdCl_3 \cdot C_5H_{10}O_5 \cdot 5H_2O$

| | |
|---|---|
| Formula | $NdCl_3 \cdot C_5H_{10}O_5 \cdot 5H_2O$ |
| Formula weight | 490.80 |
| Crystal system, space group | monoclinic, $P2(1)$ |
| $a$ (Å) | 9.138(11) |
| $b$ (Å) | 8.830(10) |
| $c$ (Å) | 9.811(11) |
| $\beta$ (°) | 94.087(18) |
| $V$ (Å$^3$) | 789.7(16) |
| $Z$ | 2 |
| $D_{calcd}$ (g/cm$^3$) | 2.064 |
| Absorption coefficient (mm$^{-1}$) | 3.832 |
| $F(000)$ | 482 |
| Crystal size (mm) | $0.30 \times 0.25 \times 0.20$ |
| $\theta$ Range for data collection (°) | 2.08–25.03 |
| Index ranges | $-10 \le h \le 10$, $-7 \le k \le 10$, $-11 \le l \le 11$ |
| Reflections collected/unique | 3237/2075 [$R_{int} = 0.0207$] |
| Completeness to $\theta = 25.03$(%) | 99.7 |
| Absorption correction | Semi-empirical from equivalents |
| Max/min transmission | 0.5145 and 0.3927 |
| Refinement method | Full-matrix least-squares on $F^2$ |
| $S$ | 1.039 |
| Final $R$ indices[$I > 2\sigma(I)$] | $R_1 = 0.0198$, $wR_2 = 0.0422$ |
| $R$ indices (all data) | $R_1 = 0.0228$, $wR_2 = 0.0429$ |
| Absolute structure parameter | 0.035(15) |
| Largest difference peak and hole (e/Å$^3$) | 0.372 and −0.350 |
| Data/restraints/parameters | 2075/579/265 |

and a chloride ion. The other two $Cl^-$ ions in the molecule are free. The three adjacent hydroxyl groups labeled $O_{(1)}H$,$O_{(2)}H$ and $O_{(3)}H$ or $O_{(2')}H$,$O_{(3')}H$ and $O_{(4')}H$ which containing the *ax–eq–ax* sequence are the coordination sites of the ribose, and the Nd–O distances at the coordination sites (from 2.445 to 2.520 Å in the β-pyranose $^1C_4$ conformation or from 2.525 to 2.67 Å in the α-pyranose $^4C_1$ conformation) are comparable to those of Pr–O (from 2.535 to 2.589 Å).[14] The ring oxygen of D-ribose does not coordinate with $Nd^{3+}$ in either molecule. All water molecules in the crystal are coordinated in the two structures.

As expected, there is an extensive network of hydrogen bonds that involve all hydroxyl groups, water molecules, and chloride ions in the crystal structure of $NdCl_3 \cdot$ribopyranose$\cdot 5H_2O$ (Table 4). The Nd–ribose molecules are organized by these hydrogen bonds and thus form a layer parallel to the plane of (1 0 −1). These layers are then also held together by hydrogen bonds with regular spaces between them. Free Cl ions distributed in the layers are responsible for the connections in the layers, and the bonding between the layers is by hydrogen bonds. The network of hydrogen bonds

Table 2
Atomic coordinates ($\times 10^4$) and equivalent isotropic displacement parameters (Å$^2 \times 10^3$) for $NdCl_3 \cdot$ribopyranose$\cdot 5H_2O$

| | $x$ | $y$ | $z$ | $U_{eq}$ |
|---|---|---|---|---|
| Nd(1) | 2776(1) | 1569(1) | 7999(1) | 25(1) |
| Cl(1) | 5637(1) | 1735(4) | 9167(1) | 40(1) |
| Cl(2) | 9638(1) | 1576(4) | 1641(1) | 41(1) |
| Cl(3) | 5452(1) | 6553(4) | 6764(1) | 43(1) |
| O(6) | 3469(4) | −1133(5) | 8306(4) | 41(1) |
| O(7) | 3194(5) | 271(5) | 5803(4) | 53(1) |
| O(8) | 4142(4) | 3177(5) | 6392(4) | 47(1) |
| O(9) | 2928(4) | 4179(5) | 8888(4) | 46(1) |
| O(10) | 2577(4) | 842(4) | 10421(3) | 42(1) |
| O(1) | 889(10) | 3025(11) | 6392(11) | 25(2) |
| O(2) | 268(19) | 2570(30) | 8908(15) | 20(3) |
| O(3) | 476(13) | 42(14) | 7439(12) | 21(3) |
| O(4) | −1904(7) | −1296(8) | 6008(6) | 28(2) |
| O(5) | −1597(12) | 2794(13) | 5505(10) | 30(2) |
| C(1) | −606(12) | 3236(13) | 6663(12) | 26(3) |
| C(2) | −944(19) | 2316(17) | 7927(13) | 25(3) |
| C(3) | −955(16) | 618(16) | 7642(12) | 24(3) |
| C(4) | −1988(15) | 252(10) | 6385(12) | 21(3) |
| C(5) | −1556(17) | 1198(13) | 5160(10) | 26(3) |
| O(1′) | −2870(8) | 2410(9) | 5197(7) | 43(2) |
| O(2′) | 1004(10) | 2483(11) | 6201(10) | 27(2) |
| O(3′) | 398(19) | 2540(30) | 8669(15) | 23(3) |
| O(4′) | 628(14) | −221(15) | 7741(12) | 27(3) |
| O(5′) | −1347(12) | 299(13) | 5363(10) | 33(3) |
| C(1′) | −1404(14) | 1904(13) | 5217(10) | 30(3) |
| C(2′) | −509(11) | 2707(13) | 6386(12) | 25(3) |
| C(3′) | −811(18) | 2020(15) | 7765(11) | 20(3) |
| C(4′) | −835(16) | 302(15) | 7749(15) | 31(3) |
| C(5′) | −1863(17) | −329(13) | 6597(13) | 36(3) |

$U_{eq}$ is defined as one third of the trace of the orthogonalized $U_{ij}$ tensor.

Table 3
Selected bond lengths (Å) and angles (°) for $NdCl_3 \cdot C_5H_{10}O_5 \cdot 5H_2O$

| | | | |
|---|---|---|---|
| *Bond lengths (Å)* | | | |
| Nd(1)–O(2′) | 2.445(10) | O(5)–C(5) | 1.450(11) |
| Nd(1)–O(9) | 2.464(5) | O(5)–C(1) | 1.455(10) |
| Nd(1)–O(3′) | 2.47(2) | C(1)–C(2) | 1.532(9) |
| Nd(1)–O(10) | 2.480(4) | C(2)–C(3) | 1.525(8) |
| Nd(1)–O(6) | 2.481(5) | C(3)–C(4) | 1.533(8) |
| Nd(1)–O(7) | 2.494(4) | C(4)–C(5) | 1.539(9) |
| Nd(1)–O(8) | 2.518(4) | O(1′)–C(1′) | 1.411(12) |
| Nd(1)–O(4′) | 2.520(14) | O(2′)–C(2′) | 1.422(10) |
| Nd(1)–O(3) | 2.525(13) | O(3′)–C(3′) | 1.442(11) |
| Nd(1)–O(1) | 2.593(10) | O(4′)–C(4′) | 1.415(11) |
| Nd(1)–O(2) | 2.67(2) | O(5′)–C(1′) | 1.425(11) |
| Nd(1)–Cl(1) | 2.782(3) | O(5′)–C(5′) | 1.441(11) |
| O(1)–C(1) | 1.423(11) | C(1′)–C(2′) | 1.534(9) |
| O(2)–C(2) | 1.432(11) | C(2′)–C(3′) | 1.525(8) |
| O(3)–C(3) | 1.431(11) | C(3′)–C(4′) | 1.517(8) |
| O(4)–C(4) | 1.420(10) | C(4′)–C(5′) | 1.523(8) |
| *Bond angles (°)* | | | |
| O(2′)–Nd(1)–O(9) | 88.0(3) | O(7)–Nd(1)–O(3) | 75.1(3) |
| O(2′)–Nd(1)–O(3′) | 61.8(4) | O(8)–Nd(1)–O(3) | 127.4(3) |
| O(9)–Nd(1)–O(3′) | 67.0(5) | O(9)–Nd(1)–O(1) | 76.7(2) |
| O(2′)–Nd(1)–O(10) | 133.4(2) | O(10)–Nd(1)–O(1) | 128.3(2) |
| O(9)–Nd(1)–O(10) | 84.80(15) | O(6)–Nd(1)–O(1) | 134.7(2) |
| O(3′)–Nd(1)–O(10) | 73.1(4) | O(7)–Nd(1)–O(1) | 80.7(3) |
| O(2′)–Nd(1)–O(6) | 123.7(3) | O(8)–Nd(1)–O(1) | 71.2(2) |
| O(9)–Nd(1)–O(6) | 148.08(12) | O(3)–Nd(1)–O(1) | 68.0(3) |
| O(3′)–Nd(1)–O(6) | 121.6(5) | O(9)–Nd(1)–O(2) | 66.4(4) |
| O(10)–Nd(1)–O(6) | 70.74(12) | O(10)–Nd(1)–O(2) | 69.0(4) |
| O(2′)–Nd(1)–O(7) | 70.3(3) | O(6)–Nd(1)–O(2) | 119.7(5) |
| O(9)–Nd(1)–O(7) | 136.67(15) | O(7)–Nd(1)–O(2) | 129.0(3) |
| O(3′)–Nd(1)–O(7) | 125.6(3) | O(8)–Nd(1)–O(2) | 119.9(5) |
| O(10)–Nd(1)–O(7) | 137.28(15) | O(3)–Nd(1)–O(2) | 61.8(5) |
| O(6)–Nd(1)–O(7) | 67.00(14) | O(1)–Nd(1)–O(2) | 59.3(4) |
| O(2′)–Nd(1)–O(8) | 72.2(3) | O(2′)–Nd(1)–Cl(1) | 146.5(2) |
| O(9)–Nd(1)–O(8) | 71.13(15) | O(9)–Nd(1)–Cl(1) | 77.14(11) |
| O(3′)–Nd(1)–O(8) | 117.1(5) | O(3′)–Nd(1)–Cl(1) | 133.7(3) |
| O(10)–Nd(1)–O(8) | 145.02(13) | O(10)–Nd(1)–Cl(1) | 75.53(9) |
| O(6)–Nd(1)–O(8) | 118.98(14) | O(6)–Nd(1)–Cl(1) | 77.10(12) |
| O(7)–Nd(1)–O(8) | 66.72(15) | O(7)–Nd(1)–Cl(1) | 100.53(12) |
| O(2′)–Nd(1)–O(4′) | 70.3(4) | O(8)–Nd(1)–Cl(1) | 74.63(12) |
| O(9)–Nd(1)–O(4′) | 130.3(3) | O(4′)–Nd(1)–Cl(1) | 141.0(3) |
| O(3′)–Nd(1)–O(4′) | 63.3(6) | O(3)–Nd(1)–Cl(1) | 149.4(3) |
| O(10)–Nd(1)–O(4′) | 79.9(3) | O(1)–Nd(1)–Cl(1) | 142.1(2) |
| O(6)–Nd(1)–O(4′) | 66.4(3) | O(2)–Nd(1)–Cl(1) | 130.5(3) |
| O(7)–Nd(1)–O(4′) | 77.9(3) | C(2)–O(2)–Nd(1) | 111.4(11) |
| O(8)–Nd(1)–O(4′) | 135.1(3) | C(2′)–O(2′)–Nd(1) | 123.6(7) |
| O(9)–Nd(1)–O(3) | 127.0(3) | C(3′)–O(3′)–Nd(1) | 112.1(12) |
| O(10)–Nd(1)–O(3) | 87.3(3) | C(4′)–O(4′)–Nd(1) | 121.6(9) |
| O(6)–Nd(1)–O(3) | 73.4(3) | C(1′)–O(5′)–C(5′) | 117.1(10) |
| C(1)–O(1)–Nd(1) | 123.9(8) | O(1′)–C(1′)–O(5′) | 110.1(9) |
| C(3)–O(3)–Nd(1) | 122.3(9) | O(1′)–C(1′)–C(2′) | 108.6(9) |
| C(5)–O(5)–C(1) | 114.7(9) | O(5′)–C(1′)–C(2′) | 111.8(7) |
| O(1)–C(1)–O(5) | 111.8(9) | O(2′)–C(2′)–C(3′) | 107.3(10) |
| O(1)–C(1)–C(2) | 109.5(11) | O(2′)–C(2′)–C(1′) | 108.2(9) |
| O(5)–C(1)–C(2) | 109.8(8) | C(3′)–C(2′)–C(1′) | 111.0(7) |
| O(2)–C(2)–C(3) | 105.8(15) | O(3′)–C(3′)–C(4′) | 109.6(13) |
| O(2)–C(2)–C(1) | 105.7(12) | O(3′)–C(3′)–C(2′) | 103.9(11) |
| C(3)–C(2)–C(1) | 111.8(8) | C(4′)–C(3′)–C(2′) | 113.1(7) |
| O(3)–C(3)–C(2) | 112.4(12) | O(4′)–C(4′)–C(3′) | 108.3(11) |
| O(3)–C(3)–C(4) | 109.2(11) | O(4′)–C(4′)–C(5′) | 114.2(13) |
| C(2)–C(3)–C(4) | 110.5(7) | C(3′)–C(4′)–C(5′) | 112.4(7) |

Table 4
Hydrogen bonds for $NdCl_3 \cdot C_5H_{10}O_5 \cdot 5H_2O$ with $H \cdots A < r(A) + 2.000$ Å and $< DHA > 110^\circ$

| D–H...A | d(D–H) | d(H···A) | d(D···A) | ∠(DHA) |
|---|---|---|---|---|
| O6–H6A···Cl3#1 | 0.840 | 2.529 | 3.185 | 135.77 |
| O6–H6B···Cl2#2 | 0.844 | 2.689 | 3.490 | 158.87 |
| O7–H7B···O5 #3 | 0.839 | 2.065 | 2.880 | 163.64 |
| O7–H7B···O1′ #3 | 0.839 | 2.104 | 2.719 | 129.83 |
| O8–H8A···Cl3 | 0.838 | 2.390 | 3.223 | 172.62 |
| O8–H8B···O4 #4 | 0.837 | 2.328 | 3.042 | 143.60 |
| O8–H8B···Cl3#2 | 0.837 | 2.782 | 3.456 | 138.78 |
| O9–H9A···Cl1#5 | 0.840 | 2.435 | 3.178 | 147.92 |
| O9–H9B···Cl2#6 | 0.840 | 2.340 | 3.174 | 172.63 |
| O10–H10A···Cl3#7 | 0.845 | 2.644 | 3.249 | 129.61 |
| O10–H10A···Cl1 | 0.845 | 2.837 | 3.232 | 110.47 |
| O10–H10B···Cl2#8 | 0.844 | 2.290 | 3.086 | 157.52 |
| O1–H1···O4 #4 | 0.930 | 1.751 | 2.660 | 164.99 |
| O2–H2···Cl2#8 | 0.930 | 2.335 | 2.917 | 120.38 |
| O3–H3···Cl2#2 | 0.930 | 2.544 | 3.195 | 127.32 |
| O4–H4···Cl3#9 | 0.820 | 2.397 | 3.201 | 167.09 |
| O2′–H2′···O5′ #4 | 0.930 | 2.403 | 2.951 | 117.54 |
| O3′–H3′···Cl2#8 | 0.930 | 2.700 | 3.162 | 111.56 |
| O4′–H4′···Cl2#2 | 0.930 | 2.093 | 2.906 | 145.30 |

Symmetry transformations used to generate equivalent atoms: #1 $x, y-1, z$; #2 $-x+1, y-1/2, -z+1$; #3 $-x, y-1/2, -z+1$; #4 $-x, y+1/2, -z+1$; #5 $-x+1, y+1/2, -z+2$; #6 $-x+1, y+1/2, -z+1$; #7 $-x+1, y-1/2, -z+2$; #8 $x-1, y, z+1$; #9 $x-1, y-1, z$.

thus forms the packed structure of the whole crystal. The $Cl^-$ ions thus play important roles not only as counterions, but also as the predominant feature in the network of hydrogen bonds.

### 3.2. IR spectroscopic study of $NdCl_3 \cdot C_5H_{10}O_5 \cdot 5H_2O$

The FT-IR spectra of D-ribose and the $Nd^{3+}$ salt are shown in Fig. 3. The absorption bands and tentative assignments are given in Table 5. The broad absorption band at around 3400 $cm^{-1}$ in the spectrum of D-ribose can be assigned to the hydrogen-bonded OH groups. This band appears broader in the spectrum of the metal complex (see Fig. 3). This observed spectral change is due to the rearrangement of the strong hydrogen-bonding network observed in the crystal structure of the complex (see Table 4). The C–H stretching vibration bands (2947, 2852, 2670, 2538 $cm^{-1}$) in the spectrum of the complex, corresponding to the band of 2928 $cm^{-1}$ in the spectrum of free D-ribose, are masked by the broaden $\nu$OH bands in the salt spectrum, and the band at 1627 $cm^{-1}$ can be assigned to the $\delta_{HOH}$ vibration of the coordinated water. The bands at 1452, 1417, 1340, 1250 $cm^{-1}$ in the spectrum of free D-ribose, which are assigned to the multiple bending vibrations of O–C–H, C–C–H, C–O–H and $CH_2$, are observed to be shifted to bands of 1456, 1408, 1315, and 1244 $cm^{-1}$ in the spectrum of the complex; the intensities become weaker upon salt formation. The characteristic vibration of the pyranose is observed in both of the spectra of D-ribose and the complex (1153 $cm^{-1}$ for D-ribose, 1152 $cm^{-1}$ for Nd–ribose). In the 1200–970 $cm^{-1}$ region, the C–O, C–C stretching vibrations and the C–O–H, C–C–O bending vibrations of D-ribose are observed to be shifted and split in the spectrum of the salt (see Table 5). Such observed splitting and shifting is indicative of the participation of the sugar hydroxyl groups in metal-

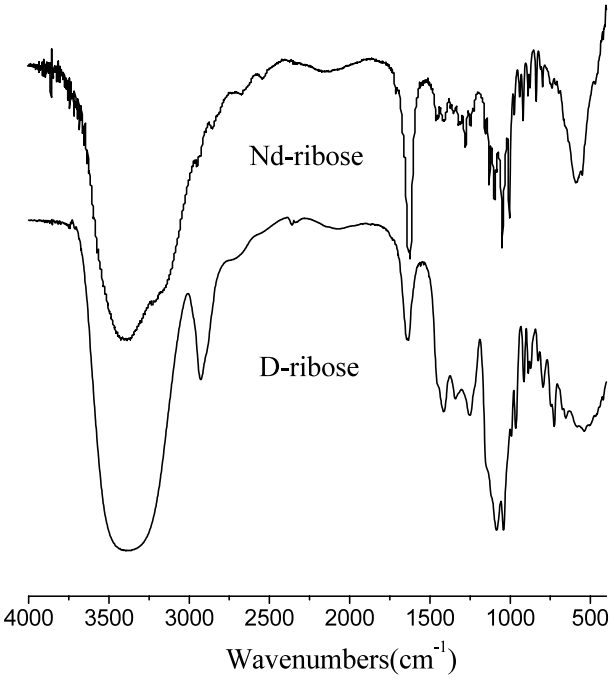


Fig. 3. The mid-IR spectra of D-ribose and Nd–ribose.

Table 5
IR data for D-ribose, Nd–ribose and Pr–ribose complex (1500–700 $cm^{-1}$)

| D-Ribose | Nd–ribose | Pr–ribose[14] | Possible assignment[32–37] |
|---|---|---|---|
| 1452 | 1456 | 1458 | $\delta OCH+\delta CCH+\delta CH_2$ |
| 1417 | 1408 | 1409 | $\delta OCH+\delta CCH$ |
| 1340 | 1315 | 1318 | $\delta OCH+\delta CCH+\delta COH$ |
| 1250 | 1244 | 1244 | $\delta CCH+\delta COH+\delta OCH$ |
| 1153 | 1153 | 1152 | $\nu C–O+\nu C–C+\delta COH$(β-pyranose) |
| 1117 | 1128 | 1128 | $\nu C–O+\nu C–C+\delta COH$ |
| 1085 | 1091 | 1095 | $\nu C–O+\nu C–C+\delta COH$ |
| 1042 | 1047 | 1048 | $\nu C–O+\nu C–C+\delta CCO$ |
| | 1003 | 1004 | $\nu C–O+\nu C–C+\delta CCO$ |
| 987 | 971 | 972 | $\nu C–O+\nu C–C+\delta CCO$ |
| 914 | 918 | 918 | $\nu C–O+\delta CCH+\nu$asy(ring of pyranose) |
| 887 | 888 | 887 | $\nu C–O+\nu C–C+\delta CCH$ |
| 872 | 874 | 874 | $\delta CH$(β-pyranose) |
| | 836 | 836 | $\delta CH$(α-pyranose) |
| 826 | | | $\delta CH$ |
| 795 | 796 | 795 | $\tau C–O+\delta CCO+\delta CCH+\nu$sy(ring of pyranose) |
| 746 | 734 | 736 | $\tau C–O+\delta CCO+\delta CCH$ |

$\delta$, bending mode; $\nu$, stretching mode; $\tau$, twisting.

ligand bonding, which therefore affect the C–O, C–C stretching vibrations and the C–O–H, C–C–O bending vibrations of the sugar moiety.

The ring skeletal deformation bands ($\delta$C–C–O and $\delta$C–C–C) of free D-ribose, mainly in the 1000–400 $cm^{-1}$ region, show considerable changes on complex formation (see Fig. 3 and Table 5). This may be attributed to distortion of the sugar ring upon metalation, although there are no published crystal data for free D-ribose for comparison with those of the complex. The spectral changes observed in this region may be interpreted as showing that metalation of the sugar perturbs the electron distribution within the sugar ring system where the vibrations are mostly localized, and causes ring distortion, resulting in the alterations in the spectrum. The 914 $cm^{-1}$ and 795 $cm^{-1}$ bands in the ribose spectrum are attributed respectively to the asymmetric and symmetric ring-breathing modes of the pyranose, and they are observed as bands at 918 and 796 $cm^{-1}$ in the spectrum of the title complex, indicating that the six-membered ring is retained in the complex. The absorption bands at about 870 and 840 $cm^{-1}$ in the pyranose spectra are generally assigned to the presence of the β and α anomers, respectively.[32,33] In relation to the spectrum of the Nd–ribose complex, the coexistence of absorption bands at 874 and 836 $cm^{-1}$ is indicative of the presence of both ribopyranose anomers in the complex. These anomers in the complex indicated by the IR data are proved by the X-ray spectroscopy.

The IR results indicate that the hydroxyl groups of D-ribose take part in the metal–oxygen interaction; the hydrogen-bond network rearranges upon metalation; the sugar moiety of the complex is D-ribopyranose in two anomeric forms and the skeleton is deformed as a result of salt formation. Since the spectrum of Nd–ribose is similar to that of Pr–ribose,[14] it may be concluded that the constitutions of the two complexes are in fact similar. The IR results are in accordance with those of X-ray spectroscopy, and the FT-IR technique is thus a useful method for detecting the formation of such complexes.

## 4. Supplementary material

Crystallographic data (without structure factors) for the structure reported in this paper have been deposited with the Cambridge Crystallographic Data Centre, CCDC No. 195540. Copies of this information may be obtained free of charge from The Director, CCDC, 12 Union Road, Cambridge CB2 1EZ, UK (Fax: +44-1223-336-033; e-mail: deposit@ ccdc.cam.ac.uk or www: http://www.ccdc.cam.ac.uk).

## References

1. Sauchelli, V. *Trace Elements in Agriculture*; Van Nostrand: New York, 1969; p 248.
2. Holm, R. P.; Berg, J. M. *Pure Appl. Chem.* **1984**, *56*, 1645–1657.
3. Predki, P. F.; Whitfield, D. M.; Sarkar, B. *Biochem. J.* **1992**, *281*, 835–841.
4. Templeton, D. M.; Sarkar, B. *Biochem. J.* **1985**, *230*, 35–42.
5. Weis, W. I.; Drickamer, K.; Hendrickson, W. A. *Nature* **1992**, *360*, 127–134.

6. Drickamer, K. *Nature* **1992**, *360*, 183–186.
7. Taylor, G. E.; Waters, J. M. *Tetrahedron Lett.* **1981**, *22*, 1277–1278.
8. Craig, D. C.; Stephenson, N. C.; Stevens, J. D. *Cryst. Struct. Commun.* **1974**, *3*, 277–281.
9. Craig, D. C.; Stephenson, N. C.; Stevens, J. D. *Cryst. Struct. Commun.* **1974**, *3*, 195–199.
10. Cook, W. J.; Bugg, C. E. *Acta Crystallogr.* **1976**, *32*, 656–659.
11. Cook, W. J.; Bugg, C. E. *J. Am. Chem. Soc.* **1973**, *95*, 6442–6446.
12. Bugg, C. E. *J. Am. Chem. Soc.* **1973**, *95*, 908–913.
13. Craig, D. C.; Stephenson, N. C.; Stevens, J. D. *Carbohydr. Res.* **1972**, *22*, 494–495.
14. Yang, L. M.; Zhao, Y.; Xu, Y. Z.; et al. *Carbohydr. Res.* **2001**, *334*, 91–95.
15. Angyal, S. J. *Pure Appl. Chem.* **1973**, *35*, 131–146.
16. Alvarez, A. M.; Desrosiers, N. M.; Morel, J. P. *Can. J. Chem.* **1987**, *65*, 2656–2660.
17. Desrosiers, N. M.; Lhermet, C.; Morel, J. P. *J. Chem. Soc., Faraday Trans.* **1991**, *87*, 2173–2177.
18. Desrosiers, N. M.; Lhermet, C.; Morel, J. P. *J. Chem. Soc., Faraday Trans.* **1993**, *89*, 1223–1228.
19. (a) Rao, C. P.; Kaiwar, S. P. *Inorg. Chim. Acta* **1991**, *186*, 11–12;
    (b) Kaiwar, S. P.; Rao, C. P. *Carbohydr. Res.* **1992**, *237*, 203–210.
20. (a) Sreedhara, A.; Raghavan, M. S. S.; Rao, C. P. *Carbohydr. Res.* **1994**, *264*, 227–235;
    (b) Sreedhara, A.; Rao, C. P.; Rao, B. J. *Carbohydr. Res.* **1996**, *289*, 39–52.
21. (a) Rao, C. P.; Kaiwar, S. P.; Raghavan, M. S. S. *Polyhedron* **1994**, *13*, 1895–1906;
    (b) Kaiwar, S. P.; Raghavan, M. S. S.; Rao, C. P. *J. Chem. Soc., Dalton Trans.* **1995**, *10*, 1569–1576.
22. Bandwar, R. P.; Rao, C. P. *Carbohydr. Res.* **1996**, *287*, 157–168.
23. (a) Rao, C. P.; Geetha, K.; Bandwar, R. P. *Bioorg. Med. Chem. Lett.* **1992**, *2*, 997–1002;
    (b) Geetha, K.; Kulshreshtha, S. K.; Rao, C. P.; et al. *Carbohydr. Res.* **1995**, *271*, 163–175.
24. Bandwar, R. P.; Sastry, M. D.; Rao, C. P.; et al. *Carbohydr. Res.* **1997**, *297*, 337–339.
25. Bandwar, R. P.; Rao, C. P. *Carbohydr. Res.* **1996**, *297*, 341–346.
26. Bandwar, R. P.; Rao, C. P.; Giralt, M.; et al. *J. Inorg. Biochem.* **1997**, *67*, 172.
27. Bandwar, R. P.; Giralt, M.; Rao, C. P. *Carbohydr. Res.* **1996**, *284*, 73–84.
28. Mukhopadhyay, A.; Kolehmainen, E.; Rao, C. P. *Carbohydr. Res.* **2000**, *324*, 30–37.
29. Mukhopadhyay, A.; Kolehmainen, E.; Rao, C. P. *Carbohydr. Res.* **2000**, *328*, 103–113.
30. Rao, C. P.; Das, T. M. *Indian J. Chem.* **2003**, *42A*, 227–239.
31. Chandrasekhar, A. *J. Imaging Technol.* **1990**, *16*, 158–161.
32. Tajmir-Riahi, A. H. *Carbohydr. Res.* **1983**, *122*, 241–248.
33. Tajmir-Riahi, A. H. *Carbohydr. Res.* **1984**, *127*, 1–8.
34. Zhang, W. J. *Biochemical Technology of Complexes of Carbohydrate*; Zhejiang University Press: Hangzhou, 1999; pp 193–198.
35. Mathlouthi, M.; Seuvre, A. M.; Koenig, J. L. *Carbohydr. Res.* **1983**, *122*, 31–47.
36. Cael, J. J.; Koenig, J. L.; Blackwell, J. *Carbohydr. Res.* **1974**, *32*, 79–91.
37. Tajmir-Riahi, A. H. *Biophys. Chem.* **1986**, *23*, 223–228.